Ion-Pair Charge-Transfer Complexes Based on (*o*-Phenylenebis(oxamato))cuprate(II) and Cyclic Diquaternary Cations of 1,10-Phenanthroline and 2,2′-Bipyridine: Synthesis, Crystal Structure, and Physical Properties

Iosu Unamuno, Juan M. Gutiérrez-Zorrilla,* Antonio Luque, Pascual Román, Luis Lezama, Rafael Calvo, and Teófilo Rojo

Departamento de Química Inorgánica, Facultad de Ciencias, Universidad del País Vasco, Apartado 644, 48080 Bilbao, Spain

Received May 8, 1998

The ion pair charge-transfer (IPCT) complexes $(C_{14}H_{12}N_2)[Cu(opba)]\cdot 3H_2O$ (**1**) and $Na_2(C_{12}H_{12}N_2)[Cu(opba)]_2\cdot 4H_2O$ (**2**), opba = *o*-phenylenebis(oxamate), have been isolated. Both compounds crystallize in the triclinic space group $P\bar{1}$. Crystal data for the compounds **1**, $a = 7.3216(13)$ Å, $b = 10.1756(9)$ Å, $c = 16.4890(16)$ Å, $\alpha = 107.786(8)°$, $\beta = 94.79(1)°$, $\gamma = 104.16(1)°$, $V = 1117.4(3)$ Å^3, $Z = 2$, $R = 0.033$ for 5332 observed reflections with $I > 3\sigma(I)$; **2**, $a = 6.732(3)$ Å, $b = 11.169(3)$ Å, $c = 12.126(2)$ Å, $\alpha = 111.01(2)°$, $\beta = 102.71(3)°$, $\gamma = 93.57(3)°$, $V = 820.1(5)$ Å^3, $Z = 2$, $R = 0.065$ for 3354 observed reflections with $I > 3\sigma(I)$. The crystal structures consist of alternated anion complex and diquaternary cation layers $\pi-\pi$ interacting through the corresponding aromatic rings. The metallic layers contain the $[Cu(opba)]_2^{4-}$ dimeric group where the copper(II) ions are in square-pyramidal environment. For both compounds an ion-pair charge-transfer (IPCT) band is observed at 517 nm. Their thermal behavior has also been explained on the basis of the different crystal arrangements. The dimeric nature of compound **1** is clearly confirmed by the observation of temperature-dependent ESR transitions between its singlet and triplet states. The $|J|$ value, determined from the positions of these transitions, is 0.085 cm^{-1} at room temperature and increases notably with decreasing temperature being 0.14 cm^{-1} at 4.2 K. Comparison of these exchange constants with those observed for other carboxylate-bridged copper compounds allow us to deduce that the temperature dependence of J is due to lattice shrinkage leading to appreciable change of the $Cu-O_{ap}$ distance. The ESR spectrum of compound **2** is characteristic of an axial g-tensor with $g_{\parallel} = 2.178$ and $g_{\perp} = 2.049$, showing a weak half-field $\Delta M_s = 2$ transition in agreement with the dimeric nature of the complex. The thermal evolution of the magnetic susceptibility corresponds to a compound with weak antiferromagnetic interactions. The best fit of the magnetic data to a dimer $S = {}^1/_2$ model gives $J = -0.8$ cm^{-1}, in good agreement with the topology of the bridging unit with the magnetic orbitals in parallel planes and a Cu−O−Cu angle of 95.4°.

Introduction

The rational design of physical properties of solids is a central topic in materials science. In the development of new materials, a fundamental requirement for the design of molecular aggregates having particular desired functions is an understanding of the magnitude and direction of the forces that exist between their constituent units. The solid-state connectivity derived from controlled assembly determines electronic band structure, magnetic structure, and polarizability. These properties are the basis of electric conductivity, bulk magnetism, and optical nonlinearities, found in numerous materials.[1] Since the discovery of the organic conductor TTF-TCNQ,[2] there has been a significant effort into the synthesis and characterization of new molecular electrically conducting materials. Yet, inorganic compounds, namely, the platinum complexes $K_2[Pt(CN)_4]X_{0.3}\cdot 3H_2O$,[3] were among the first molecular based conductors. Other inorganic systems have also been used for the preparation of materials exhibiting high conductivities including metalloporphyrins and phthalocyanine complexes,[4] DCNQI metal complexes,[5] and metal complexes of dithiolate ligands.[6]

Intermolecular charge-transfer interactions, which are a special case of the more general phenomenon of $\pi-\pi$ interac-

* To whom all correspondence should be directed.

(1) McCullough, R. D.; Belot J. A. *Chem. Mater.* **1994**, *6*, 1396.
(2) (a) Ferraris, J.; Cowan, D. O.; Walatka, V. J.; Perlstein, J. H. *J. Am. Chem. Soc.* **1973**, *95*, 948. (b) Coleman, L. B.; Cohen, M. J.; Sandman, D. J.; Yamagishi, F. G.; Garito, A. F.; Heeger, A. J. *Solid State Commun.* **1973**, *12*, 1125.
(3) Williams, J. M.; Schultz, A. J.; Underhill, A. E.; Carneiro, K. In *Extended Linear Chain Compounds*; Miller, J. S., Ed.; Plenum Press: New York, 1982; Vol. 1, pp 73−118.
(4) (a) Marks, T. J.; Kalina, D. W. In *Extended Linear Chain Compounds*; Miller, J. S., Ed.; Plenum Press: New York, 1982; Vol. 1, pp 197−331. (b) Marks, T. J. *Angew. Chem., Int. Ed. Engl.* **1990**, *29*, 857.
(5) Kobayashi, H.; Sawa, H.; Aonuma, S.; Kato, R. *J. Am. Chem. Soc.* **1993**, *115*, 7870.
(6) (a) Cassoux, P.; Valade, L.; Kobayashi, H.; Kobayashi, A.; Clark, R. A.; Underhill, A. E. *Coord. Chem. Rev.* **1991**, *110*, 115. (b) Nakamura, T.; Underhill, A. E.; Coomber, A. T.; Friend, R. H.; Tajima, H.; Kobayashi, A.; Kobayashi, H. *Inorg. Chem.* **1995**, *34*, 870. (c) Veldhuizen, Y. S. J.; Veldman, N.; Spek, A. L.; Faulmann, C.; Haasnoost, J. G.; Reedijk, J. *Inorg. Chem.* **1995**, *34*, 140. (d) Faulmann, C.; Errami, A.; Donnadieu, B.; Malfant, I.; Legros, J. P.; Cassoux, P.; Rovira, C.; Canadell, E. *Inorg. Chem.* **1996**, *35*, 3856. (e) Pullen, A. E.; Zeltner, S.; Olk, R. M.; Hoyer, E.; Abboud, K. A.; Reynolds, J. R. *Inorg. Chem.* **1996**, *35*, 4420. (f) Rovira, C.; Veciana, J.; Rubera, E.; Tarrés, J.; Canadell, E.; Rousseau, R.; Mas, M.; Molins, E.; Almeida, M.; Henriquez, R. T.; Morgado, J.; Schoeffel, J. P.; Pouget, J. P.; *Angew. Chem., Int. Ed. Engl.* **1997**, *36*, 2324. (g) Pullen, A. E.; Olk, R. M.; Zeltner, S.; Hoyer, E.; Abboud, K. A.; Reynolds, J. R. *Inorg. Chem.* **1997**, *36*, 958. (h) Veldhuizen, Y. S. J.; Smeets, W. J. J.; Veldman, N.; Spek, A. L.; Faulmann, C.; Auban-Senzier, P.; Jerome, D.; Paulus, P. M.; Haasnoost, J. G.; Reedijk, J. *Inorg. Chem.* **1997**, *36*, 4930.

10.1021/ic9805224 CCC: $15.00 © 1998 American Chemical Society
Published on Web 11/24/1998

tion, are of basic importance in many areas of chemistry. Ion-pair charge-transfer (IPCT) complexes of the type $\{A^{2+}[ML_2]^{2-}\}$ wherein the acceptor A^{2+} is a dicationic bipyridinium or phenanthrolinium derivative and $[ML_2]^{2-}$ is a planar metal dithiolene form an interesting subclass of donor−acceptor systems. The redox properties of these compounds can be tuned dependent on the metal M, the ligand L, and the nature of the acceptor cation.[7]

An additional use of molecular electronic donors and acceptors has been for the synthesis of molecular based magnetic materials.[8] In the last two decades, there has been a significant effort directed toward the preparation of bimetallic species, in which metal ions are bridged by extended bisbidentate ligands such as oxamate,[9] oxamide,[10] oxalate,[11] dithiooxalate,[12] or oximate.[13] These compounds have been of interest for both their electronic and magnetic properties.

Along the same line, Kahn et al.[14] have reported very interesting polymetallic systems, based on opba ligand, with high spin multiplicity imposing antiferro-, ferri-, and ferromagnetic interactions between nearest-neighbor magnetic centers.

The electrical, magnetic, and optical properties of highly anisotropic systems made up of stacked planar organic or organometallic units provide a focus on increasing interest for both chemist and physicists. In this context, we report in this paper, as a part of our study on IPCT materials containing the planar species $[Cu(opba)]^{2-}$ and diquaternary cations derived from phenanthroline and bipyridine, the synthesis, crystal structure, thermal behavior, and magnetic and ESR study of two new salts: 5,6-dihydropyrazino[1,2,3,4-*lmn*]-1,10-phenanthrolinium (*o*-phenylenebis(oxamato))cuprate(II) trihydrate, $(C_{14}H_{12}N_2)[Cu(opba)]\cdot 3H_2O$ (**1**), and disodium 6,7-dihydrodipyrido[1,2-a:2′,1′-c]pyrazinium bis{(*o*-phenylene bis(oxamato))-cuprate(II)} tetrahydrate, $Na_2(C_{12}H_{12}N_2)[Cu(opba)]_2\cdot 4H_2O$ (**2**).

Experimental Section

Materials. Copper(II) nitrate trihydrate $[Cu(NO_3)_2\cdot 2H_2O$, Merck], sodium hydroxide (NaOH, Fluka), 1,10-phenatholine monohydrate ($C_{12}H_8N_2\cdot H_2O$, Fluka), 2,2′-bipyridine ($C_{10}H_8N_2$, Fluka), 1,2-phenylendiamine ($C_6H_8N_2$, Fluka), 1,2-dibromoethane ($C_2H_4Br_2$, Aldrich), ethyloxalyl chloride ($C_4H_5ClO_3$, Fluka), and tetrahydrofuran (C_4H_8O, Aldrich) were used as purchased without further purification. The synthesis of the diethyl ester of the *o*-phenylenebis(oxamic acid) [Et_2H_2-(opba)],[14b] sodium (*o*-phenylenebis(oxamato))cuprate(II) trihydrate (Na_2-$[Cu(opba)]\cdot 3H_2O$),[14b] 5,6-dihydropyrazino[1,2,3,4-*lmn*]-1,10-phenanthrolinium dibromide ($C_{14}H_{12}N_2Br_2$),[15] and 6,7-dihydrodipyrido[1,2-*a*:2′,1′-*c*]pyrazinium dibromide ($C_{14}H_{12}N_2Br_2$)[16] were carried out according to the literature methods. Elemental analyses were carried out by the Microanalytical Service from the Universidad del País Vasco.

Synthesis. A general method was followed in the preparation of both compounds. To a well-stirred aqueous solution (100 mL) of Na_2-$[Cu(opba)]\cdot 3H_2O$ (0.388 g 1.0 mmol), a solution of diquaternary cation (1.0 mmol in 10 mL of water) was dropwise added. The resulting suspension was refluxed for 30 min until an almost clear solution was obtained. After filtration of any amount of insoluble material, the resulting solution was allowed to stand at room temperature, whereupon prismatic crystals of the compounds were formed.

$(C_{14}H_{12}N_2)[Cu(opba)]\cdot 3H_2O$ (1). Yield: 75%. Anal. Calcd for $C_{24}H_{16}CuN_4O_6\cdot 3H_2O$: C, 50.22; H, 3.86; N, 9.76. Found: C, 50.19; H, 3.77; N, 9.52. IR (KBr pellets, cm^{-1}): ν(C═O) 1644; γ_{oop}(opba-C−H) 862, 775; γ_{oop}(C−H) 696.

$Na_2(C_{12}H_{12}N_2)[Cu(opba)]_2\cdot 4H_2O$ (2). Yield: 80%. Anal. Calcd for $C_{16}H_{10}CuN_3NaO_6\cdot 2H_2O$: C, 41.52; H, 3.05; N, 9.08. Found: C, 42.49; H, 2.83; N, 9.63. IR (KBr pellets, cm^{-1}): ν(C═O) 1624; γ_{oop}(opba-C−H) 864, 779; γ_{oop}(C−H) 769.

Physical Measurements. Infrared spectra were obtained (KBr pellets) on a Nicolet Magna FTIR 550 spectrometer. Thermogravimetric studies were performed using 8−15 mg samples in a Setaram Tag 24 S16 instrument under a 50 mL/min flow of synthetic air; the temperature was ramped from 20 to 600 °C at a rate of 5 °C/min. A Bruker ESP300 spectrometer operating at X and Q-bands and equipped with standard Oxford low-temperature device was used to record the ESR powder spectra of the compound at different temperatures. The magnetic field was calibrated by a NMR probe, and the frequency inside the cavities was determined with a Hewlett-Packard 5352B microwave frequency

(7) (a) Kisch, H.; Dümler, W.; Chioboli, C.; Scandola, C.; Salbeck, J.; Daub, J. J. *Phys. Chem*. **1992**, *96*, 10323. (b) Kisch, H. *Coord. Chem. Rev*. **1993**, *125*, 155. (c) Kisch, H. *Comments Inorg. Chem*. **1994**, *16*, 113. (d) Nunn, I.; Eisen, B.; Benedix, R.; Kisch, H. *Inorg. Chem*. **1994**, *33*, 5079. (e) Lemke, M.; Knoch, F.; Kisch, H.; Salbeck, J. *Chem. Ber*. **1995**, *128*, 131. (f) Schmauch, G.; Knoch, F.; Kisch, H. *Chem. Ber*. **1995**, *128*, 303. (g) Hofbauer, M.; Möbius, M.; Knoch, F.; Benedix, R. *Inorg. Chim. Acta* **1996**, *247*, 147. (h) Kisch, H. *Coord. Chem. Rev*. **1997**, *159*, 385.

(8) (a) Miller J. S.; Epstein, A. J.; Reiff, W. M. *Chem. Rev*. **1988**, *88*, 201. (b) Miller J. S.; Epstein, A. J. *Angew. Chem., Int. Ed. Engl*. **1994**, *33*, 385.

(9) (a) Pei, Y., Kahn, O. *J. Am. Chem. Soc*. **1986**, *108*, 3143. (b) Pei, Y.; Verdaguer, M.; Kahn, O. *J. Am. Chem. Soc*. **1986**, *108*, 7428. (c) Ribas, J.; García, A.; Díaz, C.; Costa, R.; Yournaux, Y.; Mathonière, C.; Kahn, O.; Gleizes, A. *Inorg. Chem*. **1990**, *29*, 2041. (d) Ribas, J.; García, A.; Costa, R.; Monfort, M.; Alvarez, S.; Zanchini, C.; Solans, X.; Domenech, M. V. *Inorg. Chem*. **1991**, *30*, 841. (e) Guillou, O.; Kahn, O.; Ourhoorn, R. L.; Boubekeur, K.; Batail, P. *Inorg. Chim. Acta* **1992**, *198*−*200*, 119. (f) Baron, V.; Gillon, B.; Cousson, A.; Mathonière, C.; Kahn, O.; Grand, A.; Öhrström, L.; Delly, B.; Bonnet, M.; Boucherle, J. X. *J. Am. Chem. Soc*. **1997**, *119*, 3500.

(10) (a) Pei, Y.; Kahn, O.; Sletten, J.; Renard, J. P.; Georges, R.; Gianduzzo; J. C.; Curely, J.; Xu, Q. *Inorg. Chem*. **1988**, *27*, 47. (b) Pei, Y.; Kahn, O.; Nakatani, K.; Codjovi, E.; Mathonière, C.; Sletten, J. *J. Am. Chem. Soc*. **1991**, *113*, 6558. (c) Lloret, F.; Julve, M.; Ruiz, R.; Journaux, Y.; Najkatani, K.; Kahn, O.; Sletten, J. *Inorg. Chem*. **1993**, *32*, 27. (d) Larionova, J.; Chavan, S. A.; Yakhmi, J. V.; Froystein, A. G.; Sletten, J.; Sourisseau, C.; Kahn, O. *Inorg. Chem*. **1997**, *36*, 6374.

(11) (a) Julve, M.; Verdaguer, M.; Gleizes, A.; Philoche-Levisalles, M.; Kahn, O. *Inorg. Chem*. **1984**, *23*, 3808. (b) Bencini, A.; Bianchi, A.; Paoli, P.; Garcia-España, E.; Julve, M.; Marcelino, M. *J. Chem. Soc., Dalton Trans*. **1990**, 2213. (c) De Munno, G.; Julve, M.; Nicolo, F.; Lloret, F.; Faus, J.; Ruiz, R.; Sinn, E. *Angew. Chem., Int. Ed. Engl*. **1993**, *32*, 613. (d) Escuer, A.; Vicente, R.; Ribas, J.; Jaud, J.; Raynaud, B. *Inorg. Chim. Acta* **1994**, *216*, 139. (e) Cortés, R.; Urtiaga, M. K.; Lezama, L.; Ariortua, M. I.; Rojo, T. *Inorg. Chim. Acta* **1994**, *216*, 65. (f) Cortés, R.; Urtiaga, M. K.; Lezama, L.; Ariortua, M. I.; Rojo, T. *Inorg. Chem*. **1994**, *33*, 829. (g) Glerup, J.; Goodson, P. A.; Hodgson, D. J.; Michelsen, K. *Inorg. Chem*. **1995**, *34*, 6255. (h) Kitagawa, S.; Okubo, T.; Kawata, S.; Kondo, M.; Katada, M.; Kobayashi, H. *Inorg. Chem*. **1995**, *34*, 4790. (i) Decurtins, S.; Schmalle, H. W.; Pellaux, R.; Schneuwly, P.; Hauser, A. *Inorg. Chem*. **1996**, *35*, 1451. (j) Román, P.; Guzmán-Miralles, C.; Luque, A.; Beitia, J. I.; Cano, J.; Lloret, F.; Julve, M.; Alvarez, S. *Inorg. Chem*. **1996**, *35*, 3741. (k) Muga, I.; Gutiérrez-Zorrilla, J. M.; Luque, A.; Román, P.; Lloret, F. *Inorg. Chem*. **1997**, *36*, 743.

(12) (a) Gleizes, A.; Verdaguer, M. *J. Am. Chem. Soc*. **1981**, *103*, 7373. (b) Verdaguer M.; Gleizes, A.; Renard, J. P.; Seiden, J. *Phys. Rev. B* **1984**, *29*, 5144. (c) Trombre, J. C.; Gleizes, A.; Galy, J. *Inorg. Chim. Acta* **1984**, *87*, 129. (d) Gleizes, A.; Verdaguer, M. *J. Am. Chem. Soc*. **1984**, *106*, 3727. (e) Mitsumi, M.; Okawa, H.; Sakiyama, H.; Ohba, M.; Matsumoto, N.; Kurisaki, T.; Wakita H. *J. Chem. Soc., Dalton Trans*. **1993**, 2991.

(13) (a) Lloret, F.; Ruiz, R.; Julve, M.; Faus, J.; Journaux, Y.; Castro, I.; Verdaguer, M. *Chem. Mater*. **1992**, *4*, 1150. (b) Lloret, F.; Ruiz, R.; Cervera, B.; Castro, I.; Julve, M.; Faus, J.; Real, A.; Sapina, F.; Journaux, Y.; Colin, J. C.; Verdaguer, M. *J. Chem. Soc., Chem. Commun*. **1994**, 2615.

(14) (a) Stumpf, H. O.; Ouahab, L.; Pei, Y.; Grandjean, D.; Kahn, O. *Science* **1993**, *261*, 447. (b) Stumpf, H. O.; Pei Y.; Ouahab, L.; Le Berre, F.; Codjovi, E.; Kahn, O. *Inorg. Chem*. **1993**, *32*, 5687. (c) Stumpf, H. O.; Pei, Y.; Kahn, O.; Sletten, J.; Renard, J. P. *J. Am. Chem. Soc*. **1993**, *115*, 6738. (d) Stumpf, H. O.; Ouahab, L.; Pei, Y.; Bergerat, P.; Kahn, O. *J. Am. Chem. Soc*. **1994**, *116*, 3866. (e) Turner, S.; Michaut, C.; Kahn, O.; Ouahab, L.; Lecas, A.; Amouyal, E. *New J. Chem*. **1995**, *19*, 773. (f) Oushoorn, R. L.; Boubekeur, K.; Batail, P.; Guillou, O.; Kahn, O. *Bull. Soc. Chim. Fr*. **1996**, *133*, 777. (g) Fettouhi, M.; Ouahab, L.; Boukhar, A.; Cador, O.; Mathonière, C.; Kahn, O. *Inorg. Chem*. **1996**, *35*, 4932. (h) Pei, Y.; Turner, S. S.; Fournes, L.; Miller, J. S.; Kahn, O. *J. Mater. Chem*. **1996**, *6*, 1521.

(15) Summer, L. A. *Tetrahedron* **1968**, *24*, 5433.

(16) Homer, R. F.; Tomlinson, T. E. *J. Chem. Soc*. **1960**, 2498.

Table 1. Crystal Data and Data Collection Parameters for Compounds **1** and **2**

	compd	
	1	**2**
formula	$C_{24}H_{16}CuN_4O_6 \cdot 3H_2O$	$C_{16}H_{10}CuN_3NaO_6 \cdot 2H_2O$
M_r	574.005	462.84
system	triclinic	triclinic
space group	$P\bar{1}$	$P\bar{1}$
a (Å)	7.3216(13)	6.732(3)
b (Å)	10.1756(9)	11.169(3)
c (Å)	16.4890(16)	12.126(2)
α (deg)	107.786(8)	111.01(2)
β (deg)	94.79(1)	102.71(3)
γ (deg)	104.16(1)	93.57(3)
V (Å^3)	1117.4(3)	820.1(5)
Z	2	2
F(000)	590	470
μ(Mo Kα) (cm^{-1})	10.5	14.2
D_o (g·cm^{-3})/flotation (CCl_4/$CHBr_3$)	1.68(3)	1.88(1)
D_x (g·cm^{-3})	1.706	1.874
shape	prism	plaque
color	dark-red	dark-blue
size (mm)	0.70 × 0.40 × 0.20	0.60 × 0.60 × 0.06
temp (K)	295(1)	295(1)
θ range (deg)	1−30	1−30
indpdt reflcns	6521	4771
obsd reflcns	5332 [$I > 3\sigma(I)$]	3354 [$I > 3\sigma(I)$]
no. variables	431	267
av (Δ/σ)	0.010	0.043
S	1.76	1.49
R	0.033	0.065
R_w	0.041	0.079

counter. Magnetic susceptibility measurements were performed on powdered samples between 1.8 and 300 K with a Quantum Design MPMS-7 Squid magnetometer. The magnetic field used in the experiments was of 0.1 T, a value at which the magnetization versus magnetic field curve was still linear at 1.8 K. Experimental susceptibility values were corrected for the diamagnetic contributions and for the temperature-independent paramagnetism.

X-ray Data Collection and Structure Determination. Single-crystal collections for **1** and **2** were performed at 295 K with an Enraf-nonius CAD-4 four-circle diffractometer using graphite-monochromatized Mo Kα radiation ($\lambda = 0.710\ 69$ Å) and operating the $\omega-2\theta$ scan mode. A prismatic single crystal of **1** and a plate of **2** of dimensions 0.70 × 0.40 × 0.20 and 0.60 × 0.60 × 0.06 mm, respectively, were used for data collection. The unit cell parameters were calculated by least-squares fit of well-centered reflections on the range $9 < \theta < 13$ (**1**) and $7 < \theta < 13$ (**2**). Intensities of two reflections monitored periodically exhibited no significant variation. Data were corrected for Lorentz and polarization effects. An empirical absorption correction was applied to data following the procedure DIFABS,[17] resulting in transmission factors ranging from 0.705 to 1.262 for **1** and 0.548 to 1.762 for **2**. Neutral atom scattering factors and anomalous dispersion factors were taken from the literature.[18] Experimental details and crystal data for both compounds are given in Table 1.

The structures were solved using direct methods[19] and refined by full-matrix least-squares analysis using the X-RAY76 system.[20] In both cases, all non-hydrogen atoms were refined anisotropically except the diquaternary cation in compound **2**, which appear to be disordered with respect to a symmetry center and were isotropically refined with an occupancy factor of 0.5. Hydrogen atoms in compound **1** were located in the ΔF map and refined isotropically. For compound **2** the H atoms were placed in calculated positions, except for those of the opba ligand, whose coordinates were refined because they were clearly visible in a difference Fourier synthesis.

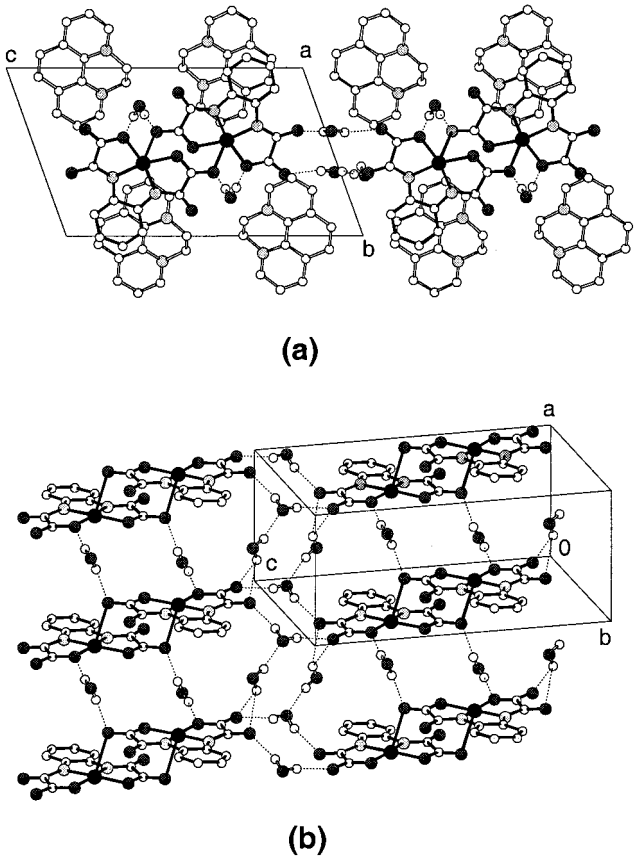

Figure 1. Compound **1**: (a) projection down the *a* axis; (b) perspective view of the anionic sublattice including H-bonding.

Results and Discussion

Synthesis. It is interesting to notice the difference in the stoichiometry of the final products even following the same procedure in the preparation. While in compound **1** a total substitution of Na^+ ions by the phenanthrolinium derivative takes place, in compound **2** only half-substitution occurs by the bipyridinium derivative even when an excess (10 times) of diquaternary bromide salt was employed. All attempts to obtain a bipyridinium derivative compound sodium free have been unsuccessful.

Crystal Structure Descriptions. $(C_{14}H_{12}N_2)$[Cu(opba)]·$3H_2O$ (1). The asymmetric unit of **1** consists of one $[Cu(opba)]^{2-}$ anion, one $(C_{14}H_{12}N_2)^{2+}$ phenanthrolinium diquaternary cation, and three water molecules. The whole structure has a definite two-dimensional character which can be viewed as an alternating sequence along the *b*-axis direction of metal complexes and organic layers interconnected by $\pi-\pi$ interactions between aromatic rings (Figure 1a).

As can be seen in Figure 1b, the metallic layer consists of dinuclear centrosymmetrical $[Cu(opba)]_2^{4-}$ groups hydrogen bonded by the water molecules.

The copper(II) ion has a 4 + 1 coordination with two nitrogen and two oxygen atoms arising from two oxamate groups in the basal plane. The square-pyramidal coordination sphere of Cu1 is completed by an apical oxygen atom O5 from the centrosymmetrically related $[Cu(opba)]^{2-}$ unit a 2.914 Å. The copper atom

(17) Walker, N.; Stuart, D. *Acta Crystallogr.* **1983**, *A39*, 158.
(18) *International Tables for X-ray Crystallography*; Kynoch: Birmingham, England, 1974; Vol. IV, p 99.
(19) Beurkens, P. T.; Admiraal, G.; Beurkens, G.; Bosman, W. P.; García-Granda, S.; Gould, R. O.; Smits, J. M. M.; Smykalla, C. *The DIRDIF program system*; Technical Report of the Crystallography Laboratory; University of Nijmegen: Nijmegen, The Netherlands, 1992.
(20) Stewart, J. M.; Machin, P. A.; Dickinson, C. W.; Ammon, H. L.; Heck, H.; Flack, H. *The X-RAY76 System*; Technol. Rep. TR-446; Computer Science Center, University of Maryland: College Park, MD, 1976.

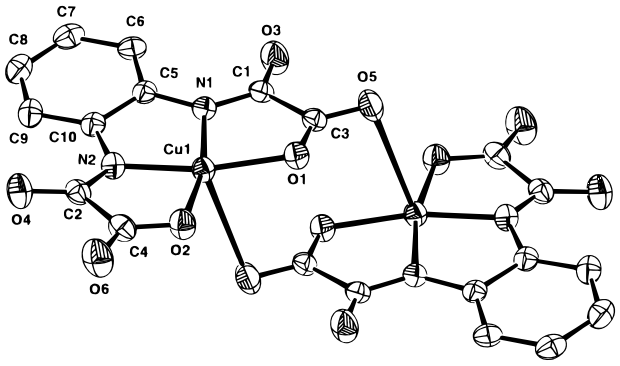

Figure 2. ORTEP view (thermal ellipsoids at the 50% probability level) of the binuclear fragment $[Cu(opba)]_2^{4-}$ in compound **1** with atom labeling.

Table 2. Selected Bond Distances (Å) and Angles (deg) for Compounds **1** and **2**

Compound **1**

	Cu1	O1	O2	N1	N2	O5[a]
O1	1.967(1)		107.37(6)	84.37(6)	167.36(7)	78.91(5)
O2	1.955(2)	3.160(2)		166.33(6)	84.3(1)	90.70(5)
N1	1.901(2)	2.598(2)			83.49(7)	98.60(6)
N2	1.920(1)		2.600(2)	2.544(2)		106.41(6)
O5[a]	2.914(2)	3.186(2)	3.528(2)	3.709(2)	3.916(2)	

Compound **2**

	Cu1	O1	O2	N1	N2	O1[b]
O1	1.967(4)		107.1(2)	84.2(2)	167.3(2)	84.6(1)
O2	1.961(4)	3.160(5)		166.4(2)	84.2(2)	86.2(1)
N1	1.906(4)	2.598(5)			83.8(2)	102.7(2)
N2	1.905(4)		2.591(5)	2.545(5)		102.3(1)
O1[b]	2.788(4)	3.259(6)	3.302(5)	3.705(5)	3.706(5)	

[a] $-x, 1-y, 1-z$. [b] $-x, -y, -z$.

is displaced from the mean basal plane toward the apical site by 0.09 Å. Two carboxylate groups bridge the two copper(II) ions through the O1 and O5 oxygen atoms involving equatorial and axial positions on the copper coordination polyhedra, respectively. This coordination behavior gives rise to the formation of a chairlike eight-membered ring Cu1−O1−C3−O5−Cu1^{I}−O1^{I}−C3^{I}−O5^{I}−Cu1 with a Cu1···Cu1^{I} distance of 5.226 Å (I: $-x, 1-y, 1-z$). A perspective view of the dinuclear unit with the atom-numbering scheme is given in Figure 2, while selected bond distances and angles are displayed in Table 2. In the metallic layer, each dimer is interconnected to the nearest six units by a hydrogen-bonding system involving the O2, O4, O5, and O6 oxygen atoms and the three water molecules, giving rise to a 2-D arrangement of groups parallel to the (1 1 0) plane, the aromatic ring of the opba ligand being parallel to the (−1 1 0) plane. Relevant hydrogen bonds are given in Table 3.

$Na_2(C_{12}H_{12}N_2)[Cu(opba)]_2\cdot 4H_2O$ (2). The unit cell of compound **2** contains two $[Cu(opba)]^{2-}$ anions, two Na^+ cations, one $(C_{12}H_{12}N_2)^{2+}$ bipyridinium diquaternary cation, and four water molecules. The crystal has a layered structure, parallel to the (1 1 0) plane, where the metallic sheets, containing $[Cu(opba)]^{2-}$ and Na^+ ions and water molecules, are separated by layers containing diquaternary cations (Figure 3). Each copper (II) ion is in a 4 + 1 surrounding. The four nearest neighbors are the O1, O2, N1, and N2 atoms from two oxamate groups; deviations from planarity less than 0.02 Å are observed for the equatorial atoms. The copper atom is lifted by 0.10 Å from the mean basal plane toward the apical donor, which is occupied by the O1^{I} atom (I: $-x, -y, -z$) belonging to the centrosymmetrically related $[Cu(opba)]^{2-}$ unit at 2.788 Å, giving rise to the dinuclear compound with an intermolecular Cu1···Cu1^{I} separation of 3.560 Å (Figure 4). The Na atom has somewhat distorted octahedral environment; the equatorial positions are occupied by the O3, O5, O4, and O6 oxygen atoms from the oxamate bridges with an average bond distance of 2.42 Å, and the axial positions, by the water molecule O01w at 2.351 Å and the O6^{II} oxygen atom at 2.510 Å (II: $1-x, 1-y, 2-z$) from a centrosymmetrically related opba ligand resulting in dimeric units with Na1···Na1^{II} distance of 3.726 Å. Selected bond distances and angles are displayed in Table 2. Water molecules are involved in hydrogen bonds around the sodium coordination sphere (Table 3).

Table 3. Hydrogen Contacts (Å, deg) for Compounds

D−H···A	D−H	D···A	H···A	D−H···A
Compound **1**				
O01w−H011···O4[a]	0.82(4)	2.825(3)	2.02(4)	165(4)
O01w−H012···O6[b]	0.77(5)	2.785(3)	2.05(5)	161(4)
O02w−H021···O2[b]	0.87(3)	2.784(2)	1.92(3)	173(4)
O02w−H022···O5	0.79(5)	2.887(3)	2.11(5)	169(5)
O03w−H031···O01w[c]	0.81(4)	2.728(3)	1.94(4)	167(4)
O03w−H032···O4	0.79(6)	3.059(3)	2.53(6)	126(5)
O03w−H032···O6	0.79(6)	3.293(3)	2.68(5)	136(5)
C7−H7···O06[d]	0.94(3)	3.436(3)	2.53(3)	164(3)
C102−H102···O5[e]	1.08(3)	3.261(3)	2.39(4)	157(3)
C103−H103···O03w[d]	0.94(3)	3.446(3)	2.52(3)	167(3)
C104−H104···O4[f]	0.88(3)	3.421(3)	2.66(4)	145(3)
C110−H110···O5[b]	0.94(3)	3.300(2)	2.38(3)	168(2)
C113−H113···O03w	0.95(4)	3.290(3)	2.41(3)	152(2)
C115−H1151···O02w	0.94(3)	3.231(3)	2.32(3)	160(3)
C116−H1161···O3	0.98(3)	3.396(3)	2.42(3)	173(2)
C116−H1162···O5[e]	0.97(4)	3.364(3)	2.51(3)	147(3)
Compound **2**				
O01w−H11···O4	0.81	3.211(8)	2.74	119
O01w−H11···O02	0.81	2.742(17)	2.15	130
O02w−H21···O4[h]	1.02	3.159(13)	2.17	160
O02w−H22···O1[i]	1.05	3.490(11)	2.45	171
C7−H7···O3[g]	0.92(12)	3.436(7)	2.59(13)	153(9)
C07−H07···O7[i]	1.02	3.165(20)	2.24	149
C08−H08···O4[j]	1.04	3.249(18)	2.35	144
C09−H09···O2[i]	1.02	3.448(17)	2.46	164
C013−H0131···O6[l]	1.03	3.441(15)	2.53	148
C013−H0132···O3[g]	0.95	3.054(17)	2.14	159
C014−H0141···O2[l]	1.03	2.961(20)	2.12	138

[a] $x+1, y, z+1$. [b] $-x+1, -y+1, -z+1$. [c] $x, y, z-1$. [d] $x-1, y-1, z$. [e] $-x, -y, -z+1$. [f] $-x, -y, -z$. [g] $-x+1, -y, -z+1$. [h] $x-1, y, z$. [i] $-x, -y, -z$. [j] $x-1, y-1, z$. [k] $x, y-1, z$. [l] $x, y, z+1$.

Therefore, the metallic layer is formed by corrugated [Cu(opba)]−Na chains running along the *b*-axis direction interconnected through the coordination sphere of copper and sodium atoms to give a 2-D arrangement of $[Cu(opba)]_2$ and $[Na_2O_8(H_2O)_2]$ dimeric groups (Figure 3).

***π*−*π* Interactions.** One interesting feature of the crystal packing for both compounds is the presence of $\pi-\pi$ interactions between the phenylene ring of opba ligand and the aromatic rings of diquaternary cations (Figure 5). The presence of this type of interactions has been evaluated,[21] and the results are shown in Table 4.

The presence of charge-transfer bands is obvious from the colors of these substances. The electronic spectra of the compounds are dominated by a broad band between 400 and 600 nm, which is responsible for the dark-red color. The λ_{IPCT} maxima for both complexes are located at 517 nm ($\epsilon = 154$

(21) Albert, A.; Cano, F. H. In *Cristalografía*; Hernández-Cano, F., Foces-Foces, C., Martínez-Ripoll, M., Eds.; Publicaciones CSIC: Madrid, 1995; p 183.

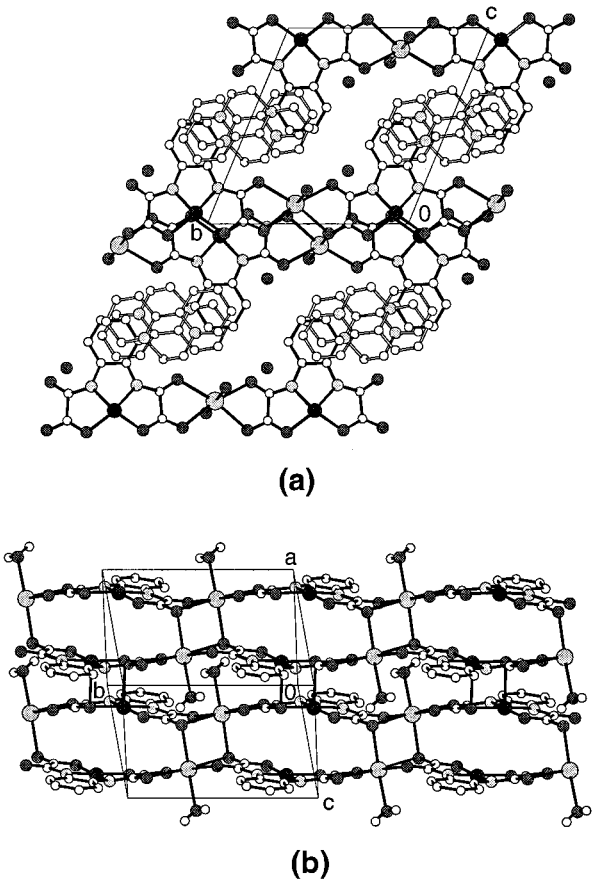

Figure 3. Compound **2**: (a) projection down the *a* axis; (b) view of the metallic layer showing the Cu(opba)−Na chains.

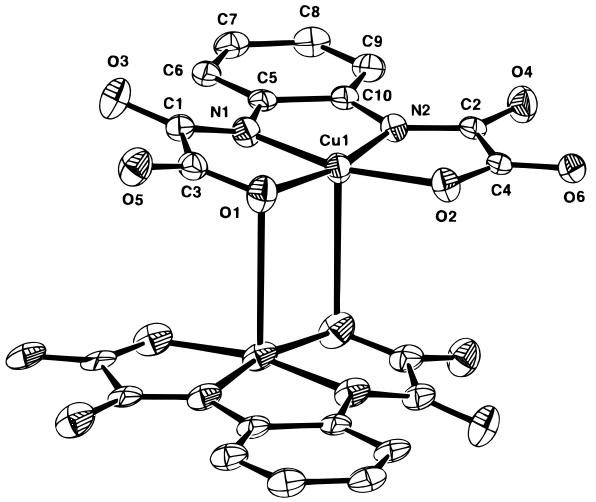

Figure 4. ORTEP view (thermal ellipsoids at the 50% probability level) of the binuclear fragment $[Cu(opba)]_2^{4-}$ in compound **2** with atom labeling.

M^{-1} cm^{-1} for **1** and 138 M^{-1} cm^{-1} for **2**) The amount of charge transfer from the donor to the acceptor is given by the parameter α^2, which can be easily calculated from absorptivity, half-bandwidth, E_{IPCT} and the distance of the two components. Values of α^2 are 2.1×10^{-3} for **1** and 2.2×10^{-3} for **2**, which are typical for outer-sphere complexes.[7d]

Thermal Behavior. Thermal decomposition of compounds starts at 50 °C with the release of water molecules. These dehydration processes are followed by steps corresponding to the oxidation of organic components, which take place at the range temperatures of 250−400 °C for **1** and 275−450 °C for **2**, giving CuO as the final residue for compound **1** and a mixture of CuO and NaO for compound **2** (Figure 6).

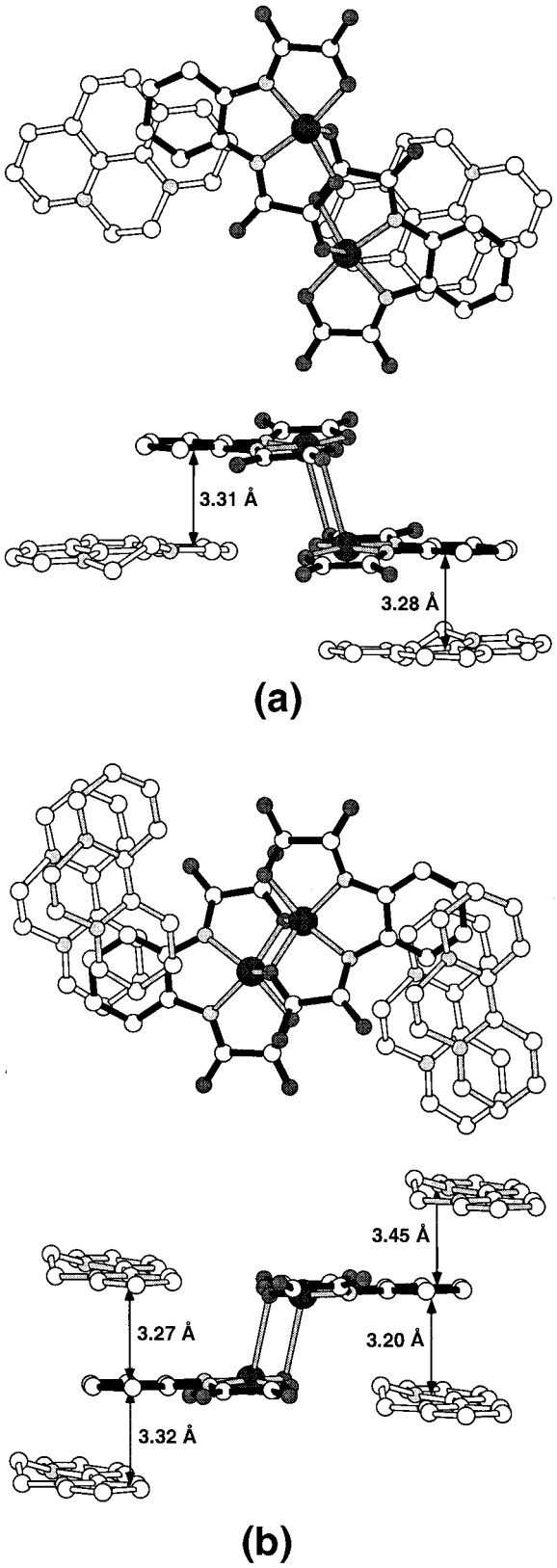

Figure 5. Top and side views of $\pi-\pi$ interactions between aromatic rings, with indication of interstacks distances: (a) compound **1**; (b) compound **2**.

It is interesting to analyze the intermediate after the dehydration processes. The anhydrous form of compound **2** is more stable than that of compound **1.** This fact can be explained

Table 4. Aromatic Ring Interactions

Compound **1**

i	j	DC	ANG	DZ	DXY	DZ'	DXY'	DS
1	2[a]	3.51	2.9	3.25	1.33	3.31	1.17	3.54
1	3[b]	3.95	1.3	3.29	2.19	3.28	2.21	3.35

[a] 1-x, y, z [b] -x, -y, -z

Ring 1: C5, C6, C7, C8, C9, C10
Ring 2: C107, C108, C109, C110, C111, N112
Ring 3: C105, C106, C107, C108, C113, C114

Compound **2**

i	j	DC	ANG	DZ	DXY	DZ'	DXY'	DS
1	2	3.51	2.5	3.32	1.14	3.27	1.28	3.46
1	2[a]	3.45	2.5	3.29	1.04	3.32	0.96	3.63
1	3[b]	3.64	5.9	3.34	1.43	3.20	1.72	3.41
1	3[c]	3.78	5.9	3.27	1.90	3.45	1.55	3.57

[a] 1+x, y , z [b] –x, –y , -z+1 [c] 1-x, -y, -z+1

Ring 1: C5, C6, C7, C8, C9, C10
Ring 2: N01, C03, C05, C07, C09, C011
Ring 3: N02, C04, C06, C08, C010, C012
DC: distance between the centroids of the aromatic rings i and j.
ANG: angle between the least-squares planes of the two rings.
DZ: distance between the centroide of j ring and the least-squares plane of i ring.
DZ': distance between the centroide of i ring and the least-squares plane of j ring
DXY: distance between the centroides of i and j projected onto the least-squares plane of i.
DXY': distance between the centroides of j and j projected onto the least-squares plane of j.
DS: distance from the centroide of I to the nearest hydrogen atom of j ring.

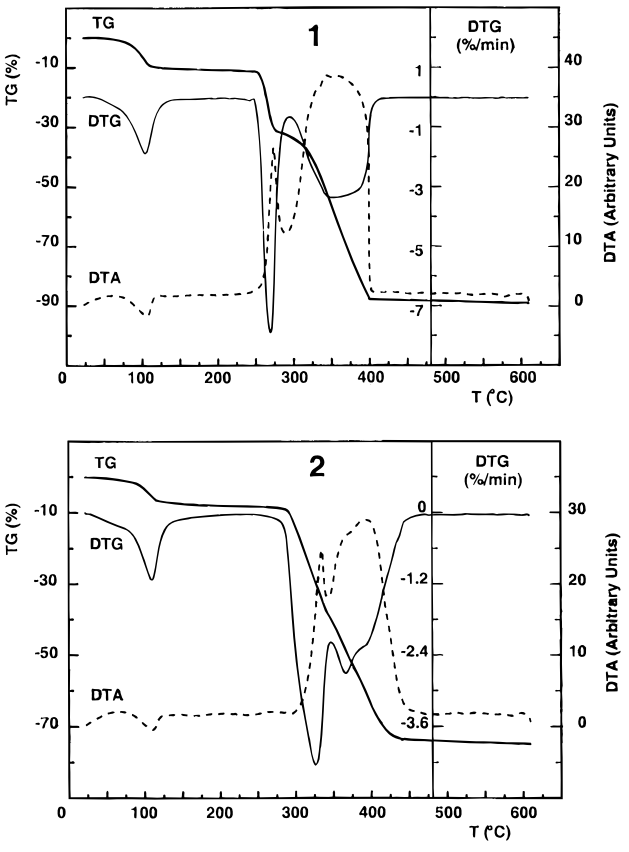

Figure 6. TG curves for the thermal decomposition of compounds **1** and **2** in synthetic air atmosphere.

because in **2** the 2-D structure remains nearly unchanged due to the Na coordination sphere, while in **1** the dehydration process means the rupture of the hydrogen bonded metallic layer.

ESR Study of Compound 1. ESR spectra for compound **1** were recorded on powdered samples in the temperature ranges 4.2−300 K and 100−300 K operating at X- and Q-bands, respectively. The obtained X-band spectra at four selected temperatures are displayed in Figure 7. The main signal (III) indicates a rhombic symmetry for the **g** tensor. From the Q-band experiments at 100 K we obtain $g_1 = 2.196$, $g_2 = 2.055$, and $g_3 = 2.031$. The observation of a g-value lower than 2.04 is not expected for a $d_{x^2-y^2}$ ground state as corresponding to a copper(II) ion in a square pyramidal geometry as exhibited in compound **1**. Moreover, the lowest *g*-value in the X-band spectra is apparently 1.987. These differences are indicative of the existence of a small zero-field splitting in a triplet state resulting from the exchange interaction between the two copper ions of the $[Cu(opba)]_2^{4-}$ units. The presence of a triplet state is confirmed by the observation of the "half-field" signal (II, $\Delta M_s = 2$) at both X- and Q-bands. At low temperatures, this signal shows an unresolved hyperfine splitting also observed on the $\Delta M_s = 1$ absorption. The approximate separation between two adjacent hyperfine lines is about 90 G, i.e., half of the expected splitting for the parallel direction in monomeric compounds and therefore in good agreement with the dimeric nature of complex **1**.

The most interesting feature of the X-band spectra is the presence of two weak signals (I, IV) symmetrically located at lower and higher fields with respect to the main signal (III). These satellite lines can be assigned as the forbidden singlet−triplet transitions, and their observation implies that the intradimeric exchange interactions (*J*) are less than the microwave quantum employed in the experiment. From the position of these signals we can deduce a $|J|$ value of 0.085 cm^{-1} at room temperature considering the spin Hamiltonian $\mathbf{H} = -2J\mathbf{S}_1\cdot\mathbf{S}_2$. When the temperature is lowered, a pronounced movement of the two singlet−triplet transitions to lower and higher fields is observed, being more significant between 300 and 50 K. This fact implies a measurable increase of the exchange interaction leading to $|J| = 0.14$ cm^{-1} at 4.2 K.

Figure 8 displays the values of $|J|$ calculated as a function of

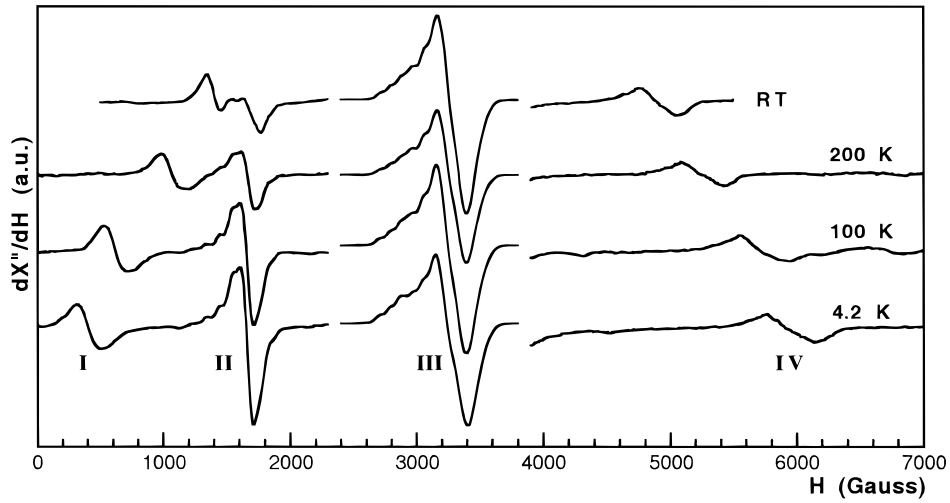

Figure 7. Temperature dependence of all visible features in the X-band ESR spectra of compound **1**.

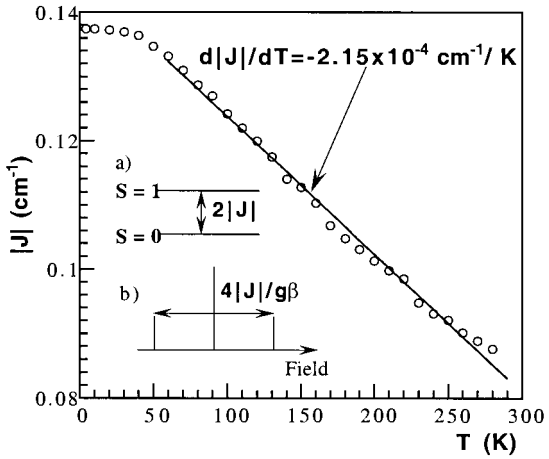

Figure 8. Thermal evolution of the $|J|$ value of compound **1**, as determined by the study of the singlet−triplet ESR transitions.

temperature T from the splitting $4|J|$ between the forbidden singlet−triplet transitions of the ESR spectrum of powdered samples. Insets a and b in this figure show respectively the definition of the exchange parameter J and sketches of the method used in this work to calculate it from the experimental results, which do not allow for obtaining its sign.

As far as we are aware, only few compounds with dimeric copper entities coupled by similar double *syn*−*anti* carboxylate bridges and Cu−Cu distances longer than 4 Å (that precludes any possible Cu−Cu direct magnetic interaction) have been previously reported.[22] These compounds exhibit weak magnetic interactions which have not been detected by magnetic susceptibility measurements. This fact can be attributed to the presence of *syn*−*anti* conformations, large $Cu-O_{ap}$ distances, and exchange pathways involving these apical positions. However, ESR studies on these compounds have shown the presence of $\Delta M_s = 2$ signals and zero-field splitting transitions, which are characteristic of triplet states. If we consider that the $Cu-O_{ap}$ distance for compound **1** (2.914 Å) is larger than those observed for similar compounds, weaker interactions should be expected for compound **1**. In this way, the singlet−triplet transitions observed in the ESR spectra (Figure 7) allowed us to determine the $|J|$ value in an accurate way. Unfortunately, the lack of magnetic data on other double *syn*−*anti* carboxylate groups preclude any discussion about the sign of the exchange interactions in these kinds of compounds.

Copper(II) compounds exhibiting single *syn*−*anti* carboxylate bridges are much more numerous. They generally present chain or layer structures with both weak ferro- and antiferromagnetic interactions.[23] In most cases, both Cu−O bonds involve equatorial oxygens giving rise to relatively large exchange couplings. However, compounds where the exchange paths are formed by carboxylate groups with the $Cu-O_{ap}-C-O_{eq}-Cu$ topology, as occurs in compound **1**, are less common and always exhibit smaller exchange interactions. Recent works on magnetic susceptibility and specific heat in copper−amino acid compounds[24] with the last type of carboxylate bridge support antiferromagnetic coupling in compound **1**. Levstein et al.[25] have shown that the magnitudes of the exchange vary linearly with the distance between the copper(II) ion and the apical oxygen. These values are about 3 orders of magnitude smaller than those measured in carboxylate-bridged copper dimers, where both Cu−O bonds involve equatorial oxygens. The correlation found by Levstein et al.[25a] was explained as a result of the competition of antiferromagnetic and ferromagnetic interactions. The positive ferromagnetic contribution to J is weakly dependent on the distance R_{ap} between copper and apical oxygen bond. The negative antiferromagnetic contribution is proportional to the overlap $S_{Cu-O} \approx \exp(-\lambda/R_{ap})$, between the copper $d_{x^2-y^2}$ and the apical oxygen sp^2 orbitals, where λ is an overlap attenuation constant, which was evaluated from the data for three copper−amino acid compounds. These results predicted a change of sign of J for copper−amino acid complexes for $R_{ap} \approx 2.75$ Å, when ferromagnetic contributions become larger than the antiferromagnetic ones.

In the case of compound **1** the exchange path involves two symmetry-related carboxylate bonds, with a distance $R_{ap} = 2.914$ Å between copper and apical oxygen. Their contributions add

(22) (a) Colacio, E.; Domínguez-Vera, J. M.; Kivekas, R.; Ruíz, J. *Inorg. Chim. Acta* **1994**, *218*, 109. (b) Dung, N.-H.; Viossat, B.; Busnot, A.; Zafra, A. G. S.; Pérez, J. M. G.; Gutiérrez, J. N. *Inorg. Chim. Acta* **1990**, *169*, 9. (c) Perlepes, S. P.; Libby, E.; Streib, W. E.; Folting, K.; Christou, G. *Polyhedron* **1992**, *11*, 923.

(23) Colacio, E.; Ruíz, J.; Moreno, J. M.; Kivekas, R.; Sundberg, M. R.; Domínguez-Vera, J. M.; Laurent, J. P. *J. Chem. Soc., Dalton Trans.* **1993**, 157 and references therein.

(24) (a) Calvo, R.; Passeggi, M. C. G.; Novak, M. A.; Symko, O. G.; Nascimento, O. R.; Terrile, M. C. *Phys. Rev. B* **1991**, *43*, 1074. (b) Rapp, R. E.; Souza, E. P. de; Godfrin, H.; Calvo, R. *J. Phys.: Condens. Matter.* **1995**, *7*, 9595.

(25) (a) Levstein, P. R.; Calvo, R. *Inorg. Chem.* **1990**, *29*, 1581. (b) Levstein, P. R.; Pastawski, H. M.; Calvo, R. *J. Phys.: Condens. Matter.* **1991**, *3*, 1877.

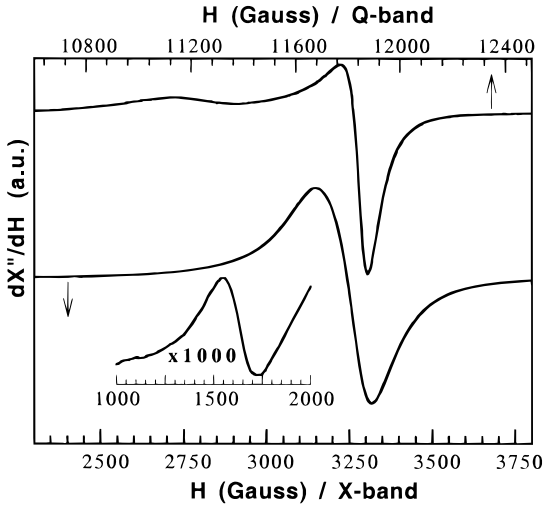

Figure 9. X- and Q-band ESR spectra of compound **2**, recorded at 100 and 4.2 K, respectively.

up to give the $|J|$ values shown in Figure 8. For double carboxylate bridges we should expect larger antiferromagnetic contributions than for the single ones and then a larger value of $|J|$ in the antiferromagnetic regime. Considering this point, the magnitude of the exchange interaction observed at room temperature, $J = 0.085$ cm^{-1} ($J/k = 0.12$ K), is then in qualitative agreement with the values for the copper−amino acid compounds. In addition, the observed temperature dependence of $|J|$ would reflect the effect of the thermal expansion of the structure. From the data given in Figure 8 we obtain $\mathrm{d}|J|/\mathrm{d}T = -2.15 \times 10^{-4}$ cm^{-1}/K for the temperature variation of $|J|$ around room temperature. Assuming $\alpha \approx 5 \times 10^{-5}$ 1/K for the linear expansion coefficient, the temperature variation of R_{ap} is $\mathrm{d}R_{ap}/\mathrm{d}T = 1.5 \times 10^{-4}$ (K)$^{-1}$. Then, attributing to thermal expansion only the temperature variation of J we get

$$\mathrm{d}|J|/\mathrm{d}(R_{ap}) \approx -1.5 \text{ cm}^{-1}/\text{Å}$$

The corresponding value obtained for carboxylate-bridged copper amino acid compounds is -0.37 cm^{-1}/Å, a factor of 4 smaller than for compound **1**. These results reflect the difference between a double and a single carboxylate superexchange path, within the uncertainties of the calculations.

The above discussion provides a simple explanation for the magnitude of the superexchange coupling observed in compound **1**. It also explains the observed temperature variation of $|J|$ as due to the change of the distance between copper and the apical oxygen ligand, because of the thermal expansion. This last result may be compared with other cases where a temperature variation of the exchange coupling was observed (see, e.g., the review paper by Hoffmann et al.[26]).

ESR and Magnetic Measurements of Compound 2. The X- and Q-bands ESR spectra for compound **2** were recorded on powdered samples between 4.2 and 300 K and are displayed in Figure 9. In the X-band spectra a quasi-isotropic signal is observed without any appreciable change in this temperature range. An extremely weak "half-field" signal is also observed at low temperatures in good agreement with the dimeric nature of the complex. The Q-band spectra show the characteristics of an axial **g**-tensor with $g_{\parallel} = 2.178$ and $g_{\perp} = 2.049$, with $G = g_{\parallel} - 2/g_{\perp} - 2 = 3.63 < 4$ according to the presence of exchange coupling. Considering the low intensity of the $\Delta M_s = 2$ transition measured at X-band, this signal was not observed in the Q-band spectra, as could be expected. These results suggest the possible presence of a weak exchange coupling of long range that could take place via hydrogen bonding.

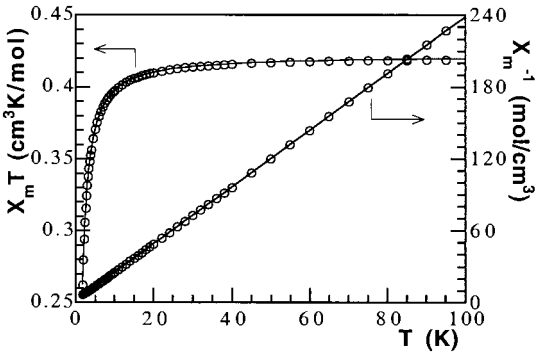

Figure 10. Thermal evolution of the reciprocal magnetic molar susceptibility and the $\chi_m T$ product, between 1.8 and 100 K.

Magnetic susceptibility measurements for compound **2** have been performed between the temperature range 1.8−300 K. Figure 10 shows the thermal variation of the reciprocal susceptibility, together with a plot of $\chi_m T$ vs T (only the data below 100 K have been represented). No remarkable accident was observed on the χ_m vs T curve. In all the recorded temperature range, the data are well described by a Curie−Weiss law ($\chi_m = C_m/T - \Theta$), with $C_m = 0.43$ cm^{3}K/mol and $\Theta = -0.9$ K. The negative Θ value, as well as the overall appearance of the $\chi_m T$ vs T curve, is indicative of the predominance of antiferromagnetic interactions in this compound. The $\chi_m T$ product lies practically constant (0.43 cm^3 K/mol) between 300 and 15 K and decreases rapidly when cooling to 1.8 K (0.26 cm^{3}K/mol).

Taking into account the crystal structure of this compound, the susceptibility data have been fitted to the Bleaney−Bowers[27] equation derived from the Heisenberg spin Hamiltonian ($\mathbf{H} = -2J\mathbf{S_1}\cdot\mathbf{S_2}$) for two coupled $S = {}^1/_2$ ions

$$\chi_m = \frac{Ng^2\beta^2}{kT}\left[\frac{1}{3 + \exp(-2J/kT)}\right]$$

The best least-squares fit (solid lines in Figure 10) is obtained with the parameter $J/k = -1.1$ K (0.8 cm^{-1}) and $g = 2.12$. The agreement factor, defined as $\mathrm{SE} = [\Phi/(n - K)]^{1/2}$, where n is the number of data points (55), K is the number of adjustable parameters (2), and Φ is the sum of squares of the residuals, is equal to 2.4×10^{-3}. Attempts to evaluate the possible interdimeric interactions by mean of a J' parameter treated in the molecular field approximation lead to extremely low values without a significant improvement of the fit.

The observed small J value is a consequence of the disposition of the copper ions in this system, with their magnetic orbitals (mainly $d_{x^2-y^2}$) in practically parallel planes, that necessarily leads to weak orbital interactions transmitted through the O1 atoms. Many examples of this kind of compounds are known but for most of them no accurate J values have been determined because of its low magnitude. Chiari et al.[28] reported a comparative study on several well-characterized compounds, from both structural and magnetic point of view, showing that the J value is strongly correlated to the Cu−O−Cu bridge.

(26) Hoffmann, S. K.; Hilczer, W.; Goslar, J. *Appl. Magn. Reson.* **1994**, *7*, 289.

(27) Bleaney, B.; Bowers, K. D. *Proc. R. Soc. London, Ser. A* **1952**, *214*, 451.

(28) Chiari, B.; Helms, J. H.; Piovesana, O.; Tarantelli, T.; Zanazzi, P. F. *Inorg. Chem.* **1986**, *25*, 2408.

However, a correlation of the exchange parameters with respect to the Cu−O_{ap} distance is difficult to be deduced. The reported *J*-values are between −1.51 and −2.15 cm^{-1} for Cu−O−Cu angles of 96.1 and 101.0°, respectively. In compound **2**, the Cu−O−Cu angle is 95.4° and the Cu−O_{ap} distance is 2.788 Å. So, the calculated *J*-value of −0.80 cm^{-1} is in good agreement with the previously described data.

As expected, the antiferromagnetic interaction decreases with the bridging angle and a crossover to ferromagnetic coupling can occur about 94° in the copper(II) dimers with this kind of bridge. Similar results have been observed for the hydroxide-bridged copper(II) dimers in which an angular dependence of *J* with a crossover point about 98° is detected.[29]

Finally, it is important to compare the structural and magnetic data of compound **2** with those of $[Cu(AE)CH_3COO]_2$ (where AE is 7-amino-4-methyl-5-aza-3-hepten-2-one)[30] in order to understand the role of the Cu−O_{ap} distance in the exchange coupling parameters. In this way, the latter compound shows a Cu−O−Cu angle of 95.3° and a *J* value of −0.50 cm^{-1}, which are similar to those of compound **2**, 95.4° and −0.80 cm^{-1}, respectively; but the Cu−O_{ap} distance is appreciably smaller (2.490 vs 2.788 Å for compound **2**). Therefore, if we consider only the orbital overlap in the interpretation of the magneto−structural correlations in this kind of compounds a decrease in the bond distance should imply an increase in the exchange coupling. Consequently, it appears that other parameters, such as the spatial disposition of the rest of the atoms concerning the bridging group, can play a more important role in the exchange pathways than that of the Cu−O_{ap} distance.

Concluding Remarks. The reaction between the planar species $[Cu(opba)]^{2-}$ and diquaternary cations, derived from phenanthroline and bipyridine, in aqueous solution affords IPCT compounds with a two-dimensional structure consisting of alternated anion complex and diquaternary cation layers $\pi-\pi$ interacting through the corresponding aromatic rings. The metallic layer in compound **1** contains the $[Cu(opba)]_2^{4-}$ dimeric group held together via a hydrogen-bonding network involving the water molecules, whereas for compound **2** the dimers are interconnected through the Na coordination sphere. This fact would explain the higher thermal stability observed for compound **2** after dehydration process.

The ESR spectra of compound **1** show the existence of small zero-field splitting in a triplet state. The observation of the two forbidden singlet−triplet transitions, which undergo pronounced shifted with temperature, allowed us to calculate the $|J|$ values accurately. These values range from 0.085 cm^{-1} at room temperature to 0.14 cm^{-1} at 4.2 K. Few compounds with dimeric entities coupled by similar double *syn*−*anti* carboxylate groups, as occurs in compound **1**, are know from a structural point of view, but the magnetic data are not reported. This fact is probably due to the small *J* values present in these types of compounds. In this way, a comparative study of magneto−structural correlations with compounds exhibiting single carboxylate bridges has been carried out. These compounds present *J* values four times smaller than those observed for compound **1** with double carboxylate bridges. The variation of *J* values with temperature of compound **1** has been explained as motivated by the change of the Cu−O_{ap} distance probably due to the thermal expansion.

Magnetic studies of compound **2** indicate the presence of antiferromagnetic interactions with a *J* value of −0.8 cm^{-1}. This small value can be explained by the weak magnetic orbital interactions (basically $d_{x^2-y^2}$) through the O1 atoms. A magneto−structural study on this kind of compound indicates that parameters such as the spatial disposition of the atoms making the bridging group can play a more important role in the exchange pathways than the metal−apical ligand distance. A crossover magnetic point can take place about 94° in the copper(II) dimers with bridging groups similar to those of compound **2**.

Acknowledgment. This work was supported by Gobierno Vasco (Grant No. PI96/69) and UPV/EHU (Grant No. 169-310-EA088/97). R.C. (on sabbatical leave from Facultad de Bioquímica y Ciencias Biológicas and INTEC (UNL-CONICET), Santa Fe, Argentina) acknowledges the Ministerio de Educación y Cultura (Spain) for financial help.

Supporting Information Available: Tables giving crystal data and details of the structure determination, atomic coordinates, anisotropic thermal parameters for non-hydrogen atoms, hydrogen atom locations, complete bond lengths and angles, and exchange pathway dimensions for **1** and **2** and reflectance and ESR spectra (14 pages). X-ray crystallographic files, in CIF format, for **1** and **2** are available on the Internet only. Ordering and access information is given on any current masthead page.

(29) Ruiz, E.; Alemany, P.; Alvarez, S.; Cano, J. *Inorg. Chem*. **1994**, *36*, 3683.
(30) Costes, J. P.; Dahan, F.; Laurent, J. P. *Inorg. Chem*. **1985**, *24*, 1018.

IC9805224